ISBN: 978-3-95450-208-0 doi:10.18429/JACoW-IPAC2019-WEPGW115

RADIATION ROBUST RF GAS BEAM DETECTOR R&D FOR INTENSITY FRONTIER EXPERMENTS

K. Yonehara†, A. Moretti, Fermi National Accelerator Lab, Batavia, USA
M. A. Cummings, R. P. Johnson[1], G. M. Kazakevich, Muons Inc, Batavia, USA

Abstract

A novel gas-filled RF beam detector is proposed that is simple and robust in high-radiation environments for future intense neutrino beam experiments. The recent result of the beam test shows a linearity of a RF test detector as a function of beam intensity.

INTRODUCTION

Fermilab is the hub institution for future intense neutrino beam experiments by using a MW-class proton driver, those facilities are called the Proton Improvement Plan II (PIP-II) [1], the Neutrino at the Main Injector (NuMI) facility [2], and the Long Baseline Neutrino Facility (LBNF) [3]. A new type of rad-hard beam monitor is needed which is located downstream of a pion-production target to align the beam with target, horns, and a far detector which is located 1,300 km away from the target in the LBNF. The beam monitor will also be used to diagnose deterioration of the target, so the monitor should have good linearity. We were supported by the Small Business Technology Transfer (STTR) grant to build a novel gas-filled RF beam detector and test its concept by using a 120 GeV/c proton beam at the Main Injector (MI) abort line [4].

All materials that have radiation sensitivity, such as ordinary coaxial cables and solid-state electronics, are placed outside of the high radiation environment. The only parts in the high radiation areas are made of aluminum, which is used to make the RF cavity body and wave guides. The cavity body is designed to be pressurized up to 2 atm. The MI beam tests were carried out in 2019. We found that the detector received integrated more than 2e15 protons without any gain change. The beam studies have demonstrated that we will not need pressurized gas to control plasma dynamics as was done in earlier Mucool Test Area (MTA) experiments [5]. Another demonstrated feature of the RF detector is that the RF signal can be calibrated without a beam calibration run. If the shunt impedance R is known, the RF power consumption is estimated with a simple $V^2/2R$ formula.

This short document shows the highlight of beam experiments during the STTR studies, evaluates the monitor performance, and discusses possible improvements for a future neutrino facility.

CONCEPT OF RF BEAM DETECTOR

When a charged beam passes through a gas-filled RF resonator it produces a large amount of ion pairs by interacting with gas. The gas permittivity in the resonator is changed proportional to the number of incident charged particles. The imaginary part of permittivity is RF power consumption in the gas plasma. The power consumption per single ion pair is given,

$$dw = 2e \int_0^{T/2} [p_e\mu_e + p^-\mu_i^- + \mu_i^+]\, E_0^2 \sin^2(\omega t)\, dt, \quad (1)$$

where μ_e and $\mu_i^{\pm}$ are the mobilities of electrons and positive (negative) ions in a gas, which is a function of $X(t) = E(t)/P = E_0/P \sin(\omega t)$, where P is a gas pressure, $E(t)$ is a RF gradient and ω is a driving angular-frequency. In the present setup, E_0/P is chosen to have a constant mobility when the beam is turned on and the RF amplitude reaches to an equilibrium condition. The coefficient p_e and p^- are the relative populations of the electrons and negative ions, respectively ($p_e + p^- = 1$). A charge recombination and electron capture processes are varied by a plasma temperature. Thus, the relative population is varied by $X(t)$ and gas species.

On the other hand, the plasma consumption is given a power equation with a RF equivalent circuit,

$$p_{gas} = \frac{V_0(V_0 - V)}{R} - CV\frac{dV}{dt}, \quad (2)$$

where R and C are a shunt impedance and capacitance of the RF cavity, respectively. The first term in the right hand side is the power gain from the RF source while the second one is the stored RF power in the cavity. At the equilibrium condition ($dV/dt = 0$), the plasma consumption power is equal to the RF power gain from the RF source.

The total number of ion pairs in the cavity can be proportional to the RF power consumption p_{gas},

$$n_{ion} \propto \frac{1}{g_c}\frac{p_{gas}}{dw}, \quad (3)$$

where g_c is the correction factor for the electric field variation over the plasma distribution. For simplicity, we assume that the beam is a zero spot size and hits on the peak gradient, thus g_c is unit in this analysis. The amount n_{ion} is proportional to the number of incident particles in the RF detector. Please note that we estimated the absolute value of n_{ion} in the past MTA experiments by using various beam detectors. To validate the concept of beam detection in the RF detector, our present setup is sufficient.

EXPERIMENT AND RESULT

Figure 1 shows the Aluminum RF test detector. It is a 2.4 GHz resonator pillbox (cylindrical) cavity. The resonator length is 75 mm. There is an end-cap flange on both ends of the detector and its center is a 1-mm thick beam window. The cavity can be pressurized up to 2 atm. An Aluminum wave guide is attached both sides of the cavity to feed RF power and extract RF signal. Gas is injected into the RF test detector through the wave guide. Thus, the wave guide can be pressurized. A dielectric pressure barrier is located

* Work supported by Fermilab Reseach Alliance, LLC under Contract No. DE-AC02-07CH11359 and DOE STTR Grant, No. DE-SC0013795.
† yonehara@fnal.gov

ISBN: 978-3-95450-208-0 doi:10.18429/JACoW-IPAC2019-WEPGW115

in a type-N adapter box which is connected other end of the wave guide.

A RF electronics is illustrated in Figure 2 for the beam test. We used a network analyzer (labeled NWA) as a RF power source which generates RF signal in the range from 0 to 20 dBm. The signal is sent through a long ½" heliax cable (Orange). There is an amplifier unit in the electric line to compensate the insertion loss of the cable. The unit consists of two amplifiers (1 W and 5 W) and two attenuators (20 dB and 10 dB), which are used to filter out RF noise and to minimize the non-linear behavior of a single amplifier. The amplified RF signal then goes through two directional couplers to measure the forward and reflected signals (White and Blue, respectively). The RF signal is sent through a 25-m-long ½" heliax cable (Red) then fed by the 1-foot-long wave guide to the input (port 1) of the 2.45 GHz gas-filled RF resonator that is used to measure the charged-particle flux. The output RF signal from the resonator is sent through another 1-foot-long wave guide and taken from the coupler (port 2). It is sufficiently long to avoid any radiation damage on the dielectric pressure barrier. Indium wire is used for all sealings.

In order to tune the quality factor (QF) of the resonator (i.e. to have the correct loaded QF), the port 2 coupler is slightly under-coupled. The output RF signal from the port 2 is then sent through a heliax cable (Green) and filtered (1.6 dB) then fed into a real-time RF power meter (RTP).

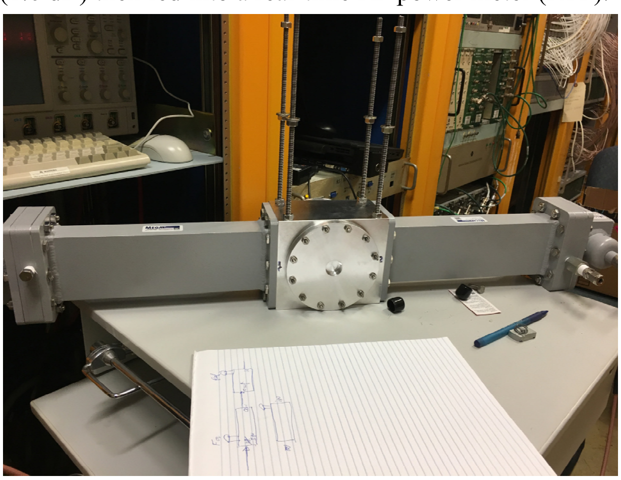

Figure 1: 2.4 GHz RF beam test detector.

Eq. (2) shows that the RF power consumption due to the beam-induced plasma can be evaluated by using the shunt impedance at the equilibrium condition. The shunt impedance can be measured from the non-beam RF signal. We measured the QF of the RF test detector with two different methods. The QF is determined from the band width, $Q = \nu_0/\Delta\nu$, where ν_0 and $\Delta\nu$ are the resonant frequency and the bandwidth, respectively. The QF can also be determined from the decay constant in the resonator, $Q = 2\pi\nu_0\tau$, where τ is the time constant (Figure 3). The discrepancy of the two measurements was less than 10 %.

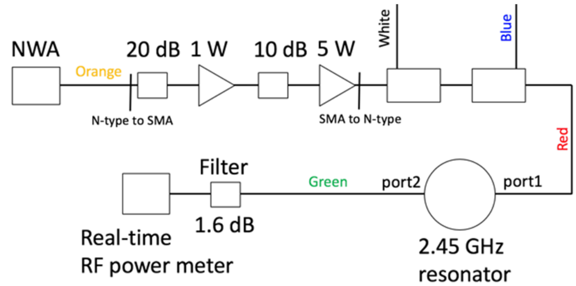

Figure 2: Schematic of RF electronics for the beam test.

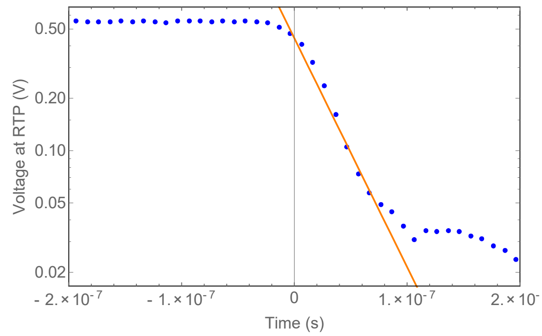

Figure 3: Observed time constant in the RF test detector.

Figure 4 shows the RF detector signal of a six-batches of the 120 GeV/c MI proton beam. The red line shows the initial RF voltage (V_0) and the blue line is the voltage at equilibrium condition (V). The RF is loaded by the beam when the beam is turned on at 0 sec. The RF recovers when the beam is turned off at 9.6 μsec. the sampling time of the detector is 10 nsec. We observed the batch gap in the RF test detector. From the signal, the gap can be 40-50 ns. This is consistent with the MI beam structure. The RF voltage fluctuates at the equilibrium condition. This may be a beating between the beam bunch timing and the RF sampling.

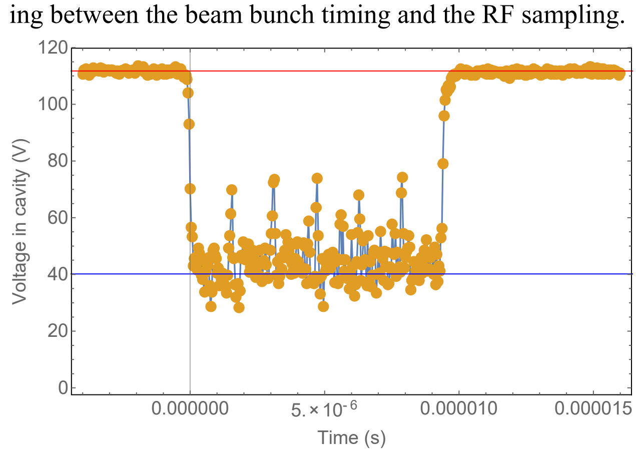

Figure 4: 1-atm N_2 gas-filled RF signal of a six-batches of the 120 GeV/c MI proton beam.

Figure 5 shows the typical beam event in the RF test detector for the linearity test. The beam is a single batched beam. Thus, the beam duration is 1.6 μs. A black solid line is the normal signal. A red and blue lines are the initial and the equilibrium RF amplitudes of the normal signal, respectively.

ISBN: 978-3-95450-208-0 doi:10.18429/JACoW-IPAC2019-WEPGW115

We sometime observed that the beam batch intensity went down by 20 % during the single spill (a black dashed line in Figure 5). This is a real time structure of the MI beam. We also demonstrated the RF power loading with an off-resonant RF driving frequency. An orange (green) line shows that the RF test detector is operated with the +2 (-2) MHz detuned driving RF frequency. When the RF power is recovered from the beam loading, the RF power is over-shooting (down-shooting) in the test cavity because of its over-coupled (under-coupled) with the RF source. It suggests that the QF can be adjusted by tuning a driving frequency. The shut impedance is changed accordingly.

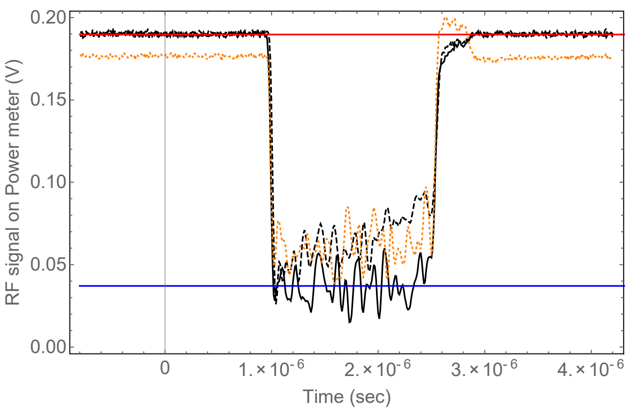

Figure 5: Four typical RF signals in the RF beam test detector with beam.

Figure 6 shows the estimated RF power consumption in the RF test detector at the equilibrium voltage by using eq. (2) where $dV/dt = 0$. The deviation of point from the fitting curve is at most 10 %. The error will be reduced by a modification which will be discussed in the next section.

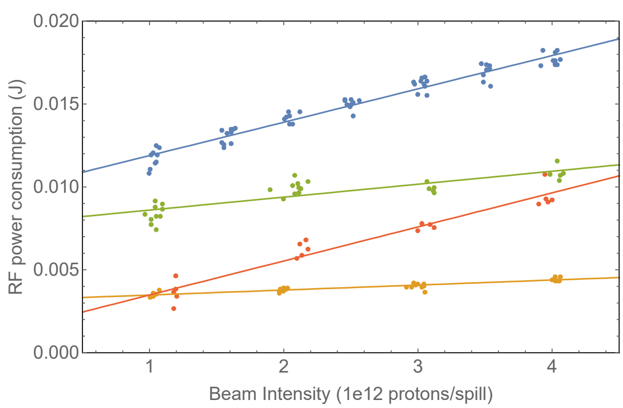

Figure 6: Estimated RF power consumption in the RF test detector. Blue is taken with atmospheric N_2 gas ($V_0 = 120\,V$), orange is taken with 2-atm N_2 gas ($V_0 = 60\,V$), green is tanek with 2-atm dry air ($V_0 = 120\,V$), and red is taken with 1-atm He gas ($V_0 = 120\,V$).

DISCUSSION

The measurement shows a good linearity of RF power consumption as a function of the beam intensity. We tested N_2, He, and dry air with varying gas pressure 1, 2 atm and excited RF voltage, 120, 90, and 60 Volts.

The deviation of points at most 10 % is found. There are several sources of the deviation. As we discussed, the beam intensity is varied in the beam spill (Figure 5). We will modify the analyzer to fix the issue. The beam position and size on the RF test detector were changed spill by spill. We observed the beam centroid and the RMS spot size by using an air SWIC but not the profile in the test run. The beam spot size is typically 20 mm in horizontal and 26 mm in vertical. It is known that the beam has a long tail. In the next run, we record the beam profile. We also noticed that the QF was changed during the beam test though we took the QF measurement just before and after the beam test. We will modify the DAQ system to take the quality factor measurement before or after the beam spill.

It should be mentioned that a fitting curve (Figure 6) does not cross the origin. We do not have any rigid model to explain this yet. An electron-ion recombination is not proportional to a plasma density. This will add a quadratic term in the RF power consumption. On the other hand, Oxygen in dry air has a large electron capture cross section and the electron capture rate is linear to the plasma density. Therefore, dry air is better option to measure the beam intensity in wider range than the present beam test. From the experimental result, we consider that a low E_0/P is good to maintain the linearity in wide beam intensity range. In order to increase the beam sensitivity, a high QF cavity is a good option. Probably, dry air is a primary gas for an intense neutrino beam application.

For a low beam intensity application, the RF beam detector can still detect the beam intensity by observing the decay time of RF amplitude. In this case, a rate equation may be solved to extract the beam intensity.

CONCLUSION

We carried out the beam demonstration test of the novel RF detector and found a good linearity of the RF response as a function of the beam intensity. We validated the concept of RF beam detector. We evaluated a possible systematic errors of the RF detector from the experimental result. Especially, the ionization in the waveguide can be a potential source of background noise. A high-Q cavity is a potential solution to mitigate the noise. We plan to study the waveguide issue by using the RF test detector. The detector will be moved to directly send a beam into the waveguide. The beam result will tell us how the RF circuit is disturbed by the plasma in the wave guide.

REFERENCES

[1] https://pip2.fnal.gov/.
[2] https://web.fnal.gov/project/TargetSystems/NuMI-AIP/_layouts/15/start.aspx#/SitePages/Home.aspx
[3] https://lbnf.fnal.gov/.
[4] K. Yonehara *et al.*, "Intense Neutrino Source Front End Beam Diagnostics System R&D", in *Proc. 9th Int. Particle Accelerator Conf. (IPAC'18)*, Vancouver, BC, Canada, Apr.-May 2018, pp. 2077-2079. doi:10.18429/JACoW-IPAC2018-WEPAK001
[5] M. Chung *et al., Phys. Rev. Lett.* Vol. 111, no. 184802, 2013.